Available online at www.sciencedirect.com
ScienceDirect
Materials Research Bulletin 43 (2008) 3088–3099
Materials Research Bulletin
www.elsevier.com/locate/matresbu

Tetragonal-$(Zr,Co)O_2$ solid solution: Combustion synthesis, thermal stability in air and reduction in H_2, H_2–CH_4 and H_2–C_2H_4 atmospheres

Felipe Legorreta Garcia, Alain Peigney, Christophe Laurent *

Institut Carnot CIRIMAT, UMR CNRS-UPS-INP 5085, Université Paul-Sabatier, 31062 Toulouse Cedex 9, France

Received 16 April 2007; received in revised form 8 November 2007; accepted 10 November 2007
Available online 19 November 2007

Abstract

The synthesis of Co^{2+}-stabilized zirconia by the nitrate/urea combustion route is investigated. Using seven times the so-called stoichiometric urea proportion allows to obtain for the first time the $Zr_{0.9}Co_{0.1}O_{1.9}$ solid solution fully stabilized in tetragonal form. The thermal stability in air and the reduction in H_2, H_2–CH_4 and H_2–C_2H_4 atmospheres are studied. The carbon forms obtained upon reduction are investigated. Reduction in H_2–CH_4 produces many carbon species including short carbon nanofibers, nanoribbons, hollow particles often forming bamboo structures, carbon-encapsulated Co particles and carbon nanotubes. Reduction in H_2–C_2H_4 produces 15–30 nm nanofibers.

Keywords: A. Oxides; A. Composites; A. Nanostructures; B. Chemical synthesis

1. Introduction

Cobalt oxides (CoO and Co_3O_4) particles dispersed on the surface of zirconia (ZrO_2) substrates are interesting catalysts [1–8]. However, the incorporation of cobalt ions into the ZrO_2 lattice and its possible role in the stabilization of the high-temperature forms of ZrO_2 is seldom mentioned. Indeed, pure ZrO_2 is found as a monoclinic phase (*m*-ZrO_2) at room temperature, but it exhibits structural transformations upon an increase of the temperature, transforming into tetragonal zirconia (*t*-ZrO_2) at approximately 1170 °C and cubic zirconia (*c*-ZrO_2) around 2370 °C [9]. It is well known that metal cations (notably Ca^{2+}, Mg^{2+}, Y^{3+} and some rare earth cations) stabilize either the tetragonal or cubic form, at increasing contents. The substitution of Zr^{4+} cations by lower valence cations is balanced by the formation of oxygen vacancies. The influence of cobalt as a stabilizer was comparatively less studied. Lick et al. [7], using an impregnation route, have reported that Co^{2+} ions stabilizes the tetragonal form and they further proposed that the incorporation of Co^{3+} ions is less probable due to its very low ionic radius (54.5 pm). However, even for the low cobalt fractions (0.2 and 2 wt%) used by these authors, the specimens still contain appreciable amounts of monoclinic phase and it was proposed that higher loadings would result in the segregation of Co_3O_4. By contrast, Choudhary et al. [6] used a coprecipitation/calcination route to prepare samples with a higher cobalt loading and reported a stabilized cubic solid solution for a Co/Zr mole ratio equal to 0.25. Maglia et al. [10] prepared mixtures of the cubic and monoclinic

* Corresponding author. Tel.: +33 5 61 55 61 22; fax: +33 5 61 55 61 63.
E-mail address: laurent@chimie.ups-tlse.fr (C. Laurent).

0025-5408/$ – see front matter
doi:10.1016/j.materresbull.2007.11.008

forms of zirconia by reacting metallic Zr and CoO. The respective proportion of these phases depends on the reaction temperature, but no information was given on the cobalt content in each phase. A study of the thermal stability in O_2 suggested that the initially cubic phase may transform into the tetragonal form upon heating and then forms *m*-ZrO_2 together with an unspecified cobalt oxide. The process is all the more pronounced when the calcination temperature is increased in the range 800–1050 °C.

In the present paper, it is proposed to investigate this topic by preparing a stabilized $Zr_{0.9}Co_{0.1}O_{1.9}$ solid solution using the nitrate/urea combustion route, which uses cheap reactants, produces gram-scale quantities of powders at the laboratory scale and can be readily upscaled. Ringuede et al. [11] have used this method for the synthesis of mixtures of CoO and Co_3O_4 with yttria-stabilized zirconia (50/50 volume fractions). The present authors have investigated the influence of the urea proportion on the formation of a nanocrystalline tetragonal $Zr_{0.9}Fe_{0.1}O_{1.95}$ solid solution [12]. In a second part of the study, the thermal stability in air of a *t*-$Zr_{0.9}Co_{0.1}O_{1.9}$ solid solution is investigated. Finally, the selective reduction of the tetragonal-stabilized $Zr_{0.9}Co_{0.1}O_{1.9}$ solid solution in H_2, H_2–CH_4 and H_2–C_2H_4 atmospheres is studied with the aim to evaluate the formation of cobalt nanoparticles and thus the potential of such a material for the formation of carbon nanotubes (CNTs). Indeed, this method has given very interesting results in the case of $Mg_{1-x}Co_xAl_2O_4$ [13] and $Mg_{1-x}Co_xO$ [14] solid solutions. To the best of our knowledge, only some results using the Fe–ZrO_2 [15] and Ni–ZrO_2 [16,17] systems have been reported in that respect.

2. Experimental

2.1. Combustion synthesis

The appropriate amounts of $Co(NO_3)_3{\cdot}9H_2O$ and $ZrO(NO_3)_2{\cdot}xH_2O$ were dissolved in deionized water (20 mL, 70 °C) with varying amounts of urea, in order to produce 5 g of $Zr_{0.9}Co_{0.1}O_{1.9}$ solid solution. The urea proportions were calculated by considering the total oxidizing valencies (V_O) and reducing valencies (V_R) of the different species [18]. The total oxidizing valencies of the nitrates is $V_O = 10.5$. The reducing valence of urea is $V_R = 6$. The molar quantity of urea (*m*) is first calculated so that the so-called stoichiometric ratio $\Phi_e = mV_R/V_O$ is equal to unity, which gives $m = 1.75$. However, as discussed by Zhang and Stangle [19], this method involves some approximations. Firstly, O_2 from the air atmosphere is not taken into account, which affects V_O. Secondly, the nitrogen-containing products are considered as being only N_2 (thus, zero is taken as the valence of nitrogen element) despite that nitrogen oxides and/or NH_3 can be formed in usually undetermined proportions. This affects both V_O and V_R. Hence it is necessary to experimentally determine the urea proportion suitable for a particular synthesis and therefore the present syntheses were performed for 10 different values of Φ_e (1–10), i.e. different values of *m* (1.75–17.5). However, for the sake of simplicity, we use the integer *n* (*n* = 1, 2, 3, 4, 5, 6, 7, 8, 9 and 10), which represents the multiplying factor rather than the molar quantity. The dish containing the solution was placed in a furnace pre-heated at 600 °C, keeping the door of the furnace open. After water evaporation, a combustion reaction takes place according to a redox reaction between the nitrates and urea, producing an oxide powder (henceforward named the as-prepared powder). The as-prepared powders will be designated as ZC-*n*U, with *n* = 1, 2, 3, 4, 5, 6, 7, 8, 9 and 10.

2.2. Thermal stability of the $Zr_{0.9}Co_{0.1}O_{1.9}$ solid solution in air

A selected specimen (ZC-7U) was chosen to perform the study of the thermal stability in air. Differential thermal analysis (DTA Netzsch 404S) was performed in flowing air (heating and cooling rates 20 °C/min up to 1300 °C). Batches of 80 mg of the powder were calcined in flowing air (4.8 L/h) at 625, 725, 825, 855, 880, 900, 925 and 1030 °C, yielding powders henceforward referred to as C625, . . ., C1030. A heating and cooling rate of 20 °C/min was applied (no dwell time at the target temperature).

2.3. Reduction of the $Zr_{0.9}Co_{0.1}O_{1.9}$ solid solution in H_2, H_2–CH_4 and H_2–C_2H_4

Batches of 1.5 g of the ZC-7U powder were reduced in H_2 atmosphere at 600, 700, 800, 900, 950 and 1000 °C, producing Co–ZrO_2 nanocomposite powders henceforward referred to as R600, . . ., R1000. Batches of 1.5 g of the powder were also reduced in H_2–CH_4 atmosphere (20 mol.% CH_4, 1000 °C) and in H_2–C_2H_4 atmosphere (40 mol.%

C_2H_4, 650 °C). For all reductions, a heating and cooling rate of 5 °C/min was applied with no dwell time at the target temperature. The total gas flow rate was equal to 15 L/h and the gas was dried on P_2O_5.

2.4. Characterization

Room temperature powder X-ray diffraction (XRD) patterns were obtained with a Brüker D4 endeavor diffractometer using Cu Kα radiation. The proportions of tetragonal and monoclinic zirconia phases were evaluated from the XRD patterns using a method similar to that reported by Garvie and Nicholson [20]. Specific surface area measurements were performed using N_2 adsorption at liquid N_2 temperature in a Micromeritics Flow Sorb II 2300 apparatus (BET method). This instrument gives a specific surface area value from one point (*i.e.* one adsorbate pressure) and requires calibration. The reproducibility of the results was determined to be in the ±3% range. The carbon content in the as-prepared powders and in the powders obtained after reduction in H_2–CH_4 and H_2–C_2H_4 was determined by flash combustion with an accuracy of ±2%. Selected oxide powders were observed by scanning electron microscopy (SEM JEOL JSM 6400). Selected reduced powders were observed by field-emission gun scanning electron microscopy (JEOL JSM 6700F) and transmission electron microcopy (JEOL 200CX).

3. Results and discussion

3.1. Combustion synthesis

The dish containing the nitrate/urea solution is introduced in the furnace pre-heated at 600 °C. Water evaporation is observed, the furnace temperature diminishing by about 40 °C before increasing again to 600 °C. Then the combustion takes place according to a redox reaction between the nitrates and urea. Neither red fumes characteristic of NO_2 formation nor the characteristic smell of ammonia was detected for any synthesis. For ZC-1U, the combustion reaction is not violent and is accompanied by a red flame. For ZC-2U, and notably for ZC-3U, the reaction is much more violent and is accompanied by a strong yellow flame, whereas for ZC-4U, the reaction is milder but still with a yellow flame. All four combustion products are not homogeneous in color. For samples with n = 5–10, the process is much milder and there is simply an incandescence of the material and no flame. All six combustion products are homogeneous in color. The measured temperature of the furnace during the combustion (Fig. 1a) varies very little except for n = 3, reflecting the visual observations. Note that the maximum temperature reached in the vessel is probably higher than that recorded for the furnace. The total time from dish introduction to end of reaction increases with n (Fig. 1b). There is a gap between ZC-4U (2.5 min) and ZC-5U (6.8 min). This time increase reflects the increase of the water evaporation duration due to a more sluggish solution when the urea content is increased and also the fact that the process is slower when there is no flame (*i.e.* for n = 5–10). Similar results have been obtained for the synthesis of $Zr_{0.9}Fe_{0.1}O_{1.95}$ [12].

It was verified that the as-prepared powders contain only trace amounts of carbon. The BET specific surface area (S_w, Fig. 2) tends to increase when the urea content is increased, but it could also be possible to separate the specimens into two groups, with S_w in the range 7–17 m^2/g for n = 1–5 and S_w in the range 23–30 m^2/g for n = 6–10. These groups almost match those observed above except that powder ZC-5U now falls in the first one. The higher S_w for the second group of powders could reflect a smaller grain size, due to both the milder nature of the combustion process and the increasing expansion of the powder due to the higher release of gases for higher urea contents.

The XRD patterns of the as-prepared powders are shown in Fig. 3. Tetragonal zirconia is the major phase detected for n = 1–4 and the only one for n = 5–10. Monoclinic zirconia is also detected, extremely faintly for ZC-1U and ZC-4U but very clearly for ZC-2U and ZC-3U, where it accounts for 40 and 23%, respectively, with respect to all zirconia phases. A very wide (3 1 1) peak of Co_3O_4 is faintly detected for ZC-2U, ZC-3U and ZC-4U, and also possibly for ZC-9U and ZC-10. The (1 0 1) peak of the tetragonal phase appears to be slightly shifted to the high 2θ-side for ZC-7U compared to the other powders, which could reveal a higher Co^{2+} content in the tetragonal zirconia phase for ZC-7U. It is further noticed that the diffraction peaks of the tetragonal phase are quite narrow for n = 1–3 and much broader for n = 4–10, ZC-7U showing the broadest peaks. This could reflect a trend for a decreasing crystallite size upon the increase in urea proportion, in agreement with the BET S_w data.

Typical low-magnification SEM images of the as-prepared powders are shown in Fig. 4a and b. The powders are made up of large grains, measuring several tens of micrometers across, as well as micro- or submicrometric grains. It

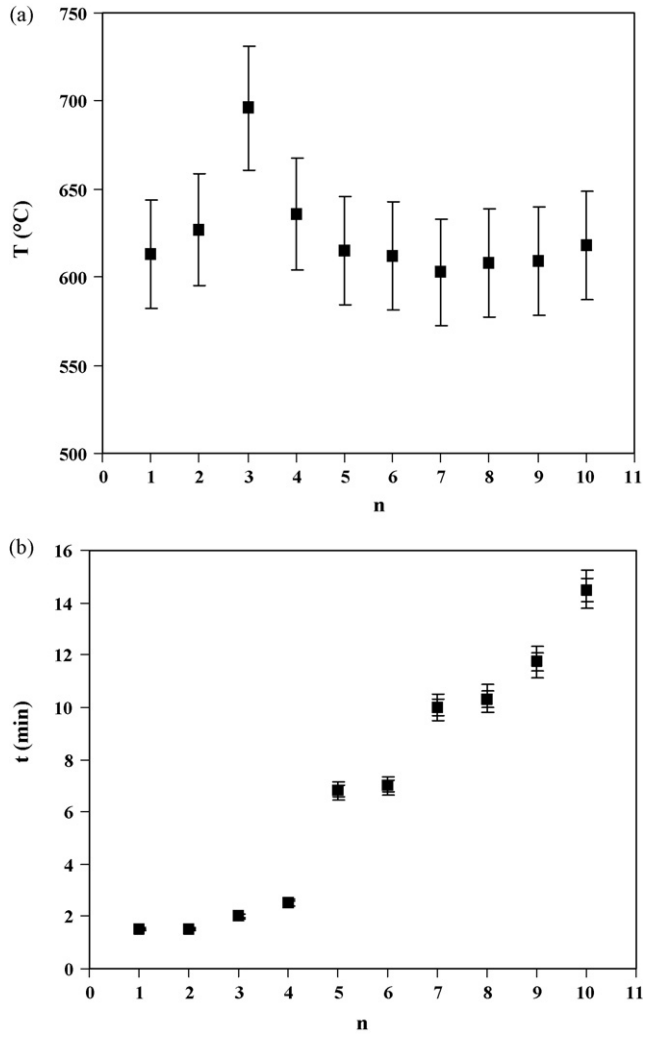

Fig. 1. Temperature reached by the furnace during combustion in a furnace pre-heated at 600 °C (a) and time for completion of reaction (b) vs. the proportion of urea (n) used for the combustion synthesis.

was observed in the case of (Zr,Fe)O_2 powders [12], the proportion of the latter ones tends to increase upon the increase of the urea proportion due to the higher expansion occurring during the combustion reaction. Furthermore, the zirconia grains are quite porous, reflecting the escaping of gases during the combustion. Higher magnification SEM images (Fig. 4c and d) illustrate typical areas found in the powders: fairly dense flat surfaces, partly broken due to the escaping of gases (Fig. 4c) and much more porous areas, revealing crystallites not larger than 100 nm (Fig. 4d). A previous study [12] revealed a trend towards a decrease in the average crystallite size upon the increase of the urea proportion. This is in broad agreement with the present SEM, XRD and S_w results.

Using a low urea proportion (n = 1–4) produces powders which are neither homogeneous samples nor monophased zirconia, possibly because the maximal temperature reached during the combustion is not the same throughout the sample. For higher values of n (n = 5–8), the milder and significantly longer combustion allows to obtain the $Zr_{0.9}Co_{0.1}O_{1.9}$ solid solution stabilized in the tetragonal form, no free cobalt oxide being detected. It is possible that the crystallite size of the zirconia species plays an important role as larger crystallites will more easily end up in the form of the stable monoclinic form. Increasing the urea proportion favors the emission of gases and therefore the expansion of the solid phase, which favors the formation of smaller crystallites. This could explain why no monoclinic zirconia is detected for n = 5–10. These experimental conditions could also favor the formation of suitable gel-like species by formation of complex of the zirconium and cobalt ions with urea, which could in turn trigger the direct incorporation of

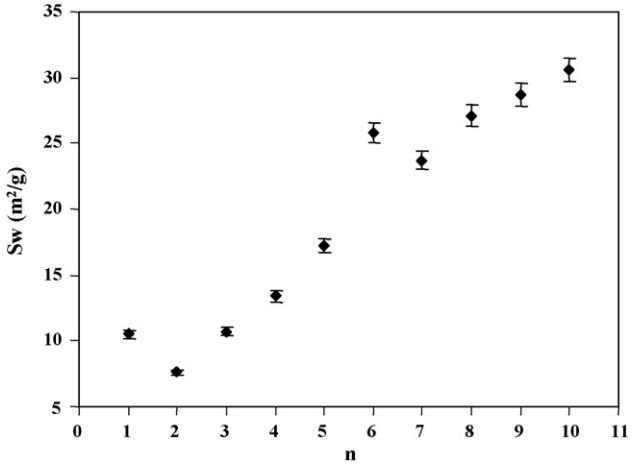

Fig. 2. Specific surface area of the as-prepared powders vs. the proportion of urea (n) used for the combustion synthesis.

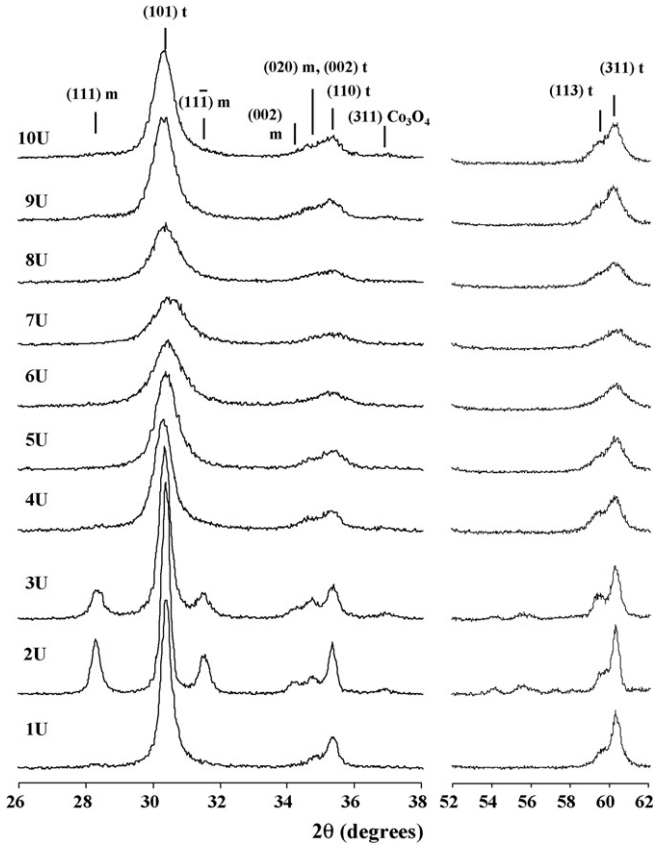

Fig. 3. XRD patterns of the as-prepared powders. The proportion of urea used for the combustion is indicated as 1U, 2U, . . ., 10U.

the cobalt ions in the zirconia phase and therefore favor crystallization in stabilized form at moderate temperature. Further studies, notably on all intermediate species, would be required to totally elucidate the involved mechanisms.

The powder ZC-7U, which is considered to be the desired tetragonal $Zr_{0.9}Co_{0.1}O_{1.9}$ solid solution, was selected for further studies.

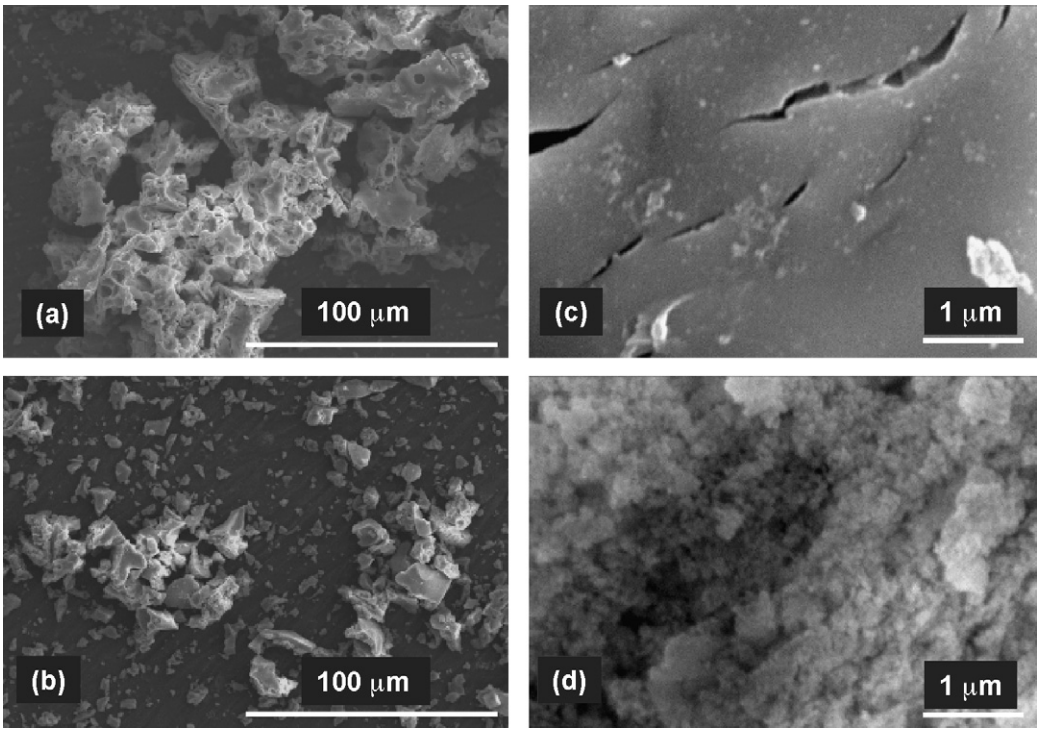

Fig. 4. SEM images of some as-prepared powders synthesized with different urea proportions (n): (a) $n = 4$; (b) $n = 7$; (c) $n = 4$; (d) $n = 10$.

3.2. Thermal stability of the tetragonal $Zr_{0.9}Co_{0.1}O_{1.9}$ solid solution in air

The thermal stability of the tetragonal $Zr_{0.9}Co_{0.1}O_{1.9}$ solid solution was investigated by DTA. The DTA curve (not shown) revealed endothermic peaks at 940 and 1194 °C upon heating and exothermic peaks at 915 and 800 °C upon cooling. The DTA curve of a cobalt-free tetragonal ZrO_2 powder prepared in the same conditions for the sake of comparison showed an endothermic peak at 1193 °C upon heating and a exothermic peak at 857 °C upon cooling. The room temperature XRD patterns of the powders after calcination in air at different temperatures (625, 725, 825, 855, 880, 900, 925 and 1030 °C) are shown in Fig. 5. For powders C625 and C725, only the peaks of the tetragonal solid solution are detected, as in the as-prepared powder. For higher calcination temperatures, Co_3O_4 and m-ZrO_2 are detected as well, the proportion of the latter phase markedly increasing at the expense of the tetragonal phase upon the increase of calcination temperature (Fig. 6). For C625–C855, the (1 0 1) peak accounting for the tetragonal phase is progressively more narrow, indicating some crystallite growth. Moreover, for C625, C725 and C825, the position of this peak gradually shifts to lower 2θ angles, i.e. revealing that the corresponding inter-reticular distance is progressively higher, which could indicate that the tetragonal phases contains less and less Co^{2+} ions. This could reveal that the phase partitioning from the cobalt-stabilized tetragonal solid solution to the mixture of m-ZrO_2 and Co_3O_4 takes place at temperatures as low as 625 °C. Free Co_3O_4 could remain undetected on the XRD patterns because of a very small size. The presence of free Co_3O_4 thus accounts for the DTA peaks at 940 °C (heating) and 915 °C (cooling), which represent the reversible transformation of this phase into CoO. This is in agreement with previous results [14]. The DTA peaks at 1194 °C (heating) and 800 °C (cooling) therefore, respectively represent the monoclinic-to-tetragonal (heating) and tetragonal-to-monoclinic (cooling) transformations of ZrO_2. As could be expected, the specific surface area of the powders decreases with increasing calcination temperature (*ca.* 24, 12.7, 3.5, 3.1, 1.8 and 1.4 m^2/g for the as-prepared, C625, C725, C825, C855 and C1030 powders, respectively). The main part of the decrease principally takes place prior to both the formation of Co_3O_4 in detectable amounts and the transformation of the zirconia phase and could reflect the crystallite growth of the tetragonal phase, as indicated by XRD data. The above data show that the thermal stability in air of the $Zr_{0.9}Co_{0.1}O_{1.9}$ solid solution is lower than that of a $Zr_{0.9}Fe_{0.1}O_{1.95}$ solid solution, which was shown [12] to be stable up to about 875 °C.

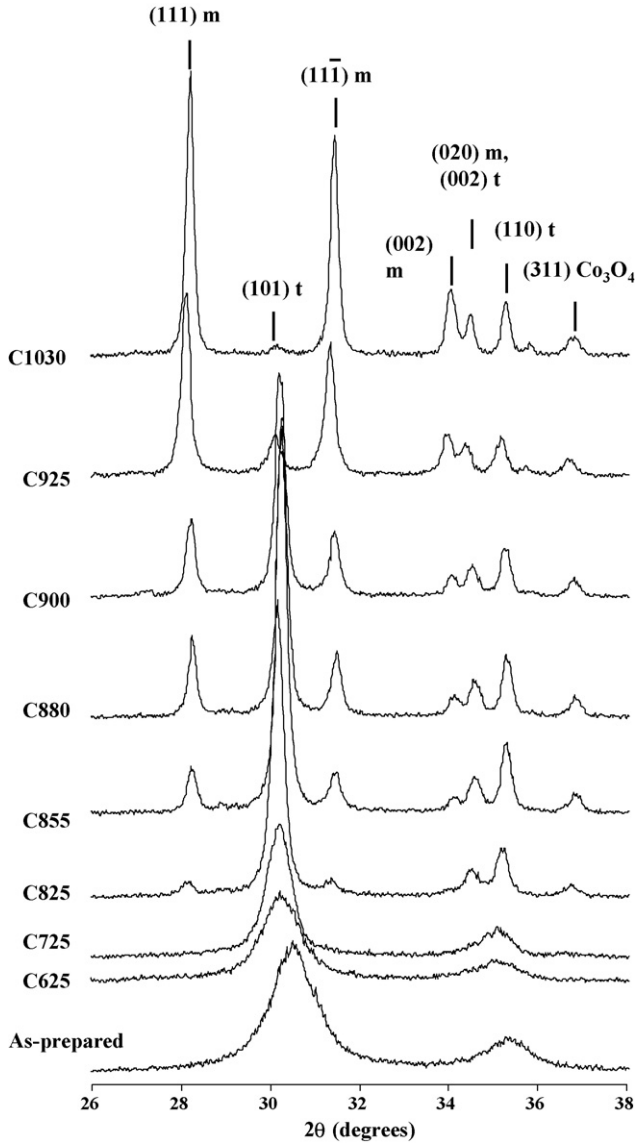

Fig. 5. Room temperature XRD patterns of the powders after calcination in air at different temperatures.

3.3. Reduction of the $Zr_{0.9}Co_{0.1}O_{1.9}$ solid solution in H_2, H_2–CH_4 and H_2–C_2H_4

The tetragonal $Zr_{0.9}Co_{0.1}O_{1.9}$ solid solution was reduced in H_2 atmosphere at 600, 700, 800, 900, 950 and 1000 °C producing Co–ZrO_2 nanocomposite powders (R600, . . ., R1000). The XRD pattern (not shown) of R600 is identical to that of the starting powder, i.e. only the tetragonal solid solution is detected. For R700 and R800, the (1 1 1) peak of face-centered-cubic cobalt (ε-Co) is very faintly detected besides the tetragonal solid solution. For powders R900, R950 and R1000, the ε-Co(1 1 1) peak is detected with an increasing intensity upon the increase in reduction temperature and *m*-ZrO_2 is also detected. The latter phase represents 14, 67 and 83% of all zirconia phases for R900, R950 and R1000, respectively, which is slightly less to what is observed upon calcinations in air (Fig. 6). These results could reflect that the reduction of the Co^{2+} ions to form metallic Co, in H_2 atmosphere, takes place at slightly higher temperatures than does the phase partitioning in air because the latter involves the oxidation of Co^{2+} in Co^{3+} which is probably easy. It is nevertheless probable that some Co nanoparticles are formed when the reduction is performed at 600 °C, even though ε-Co is not detected on the XRD pattern for R600. Indeed, a Mössbauer spectroscopy study of the

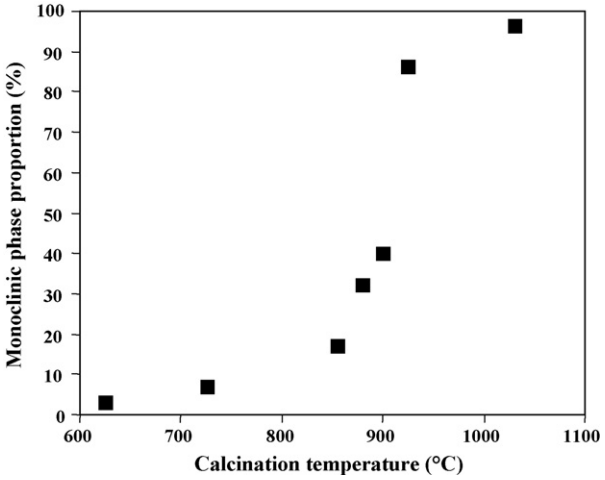

Fig. 6. Proportion of monoclinic zirconia (with respect to all zirconia phases) evaluated from the XRD patterns vs. the calcination temperature.

powder formed by H_2 reduction at 600 °C of a tetragonal $Zr_{0.9}Fe_{0.1}O_{1.95}$ solid solution revealed the presence of α-Fe, which was not detected on the corresponding XRD pattern despite a size in the range 10–50 nm as evaluated from FEG-SEM observations [21]. Moreover, Choudhary et al. [6] showed that mobility of lattice oxygen in Co^{2+}-stabilized cubic zirconia is higher than in Fe^{3+}-stabilized cubic zirconia, thus favoring the reduction to the metallic phase.

The tetragonal $Zr_{0.9}Co_{0.1}O_{1.9}$ solid solution was reduced in H_2–CH_4 atmosphere (20 mol.% CH_4) at 1000 °C. The XRD pattern (not shown) is similar to that of powder R1000, monoclinic zirconia representing 88% of all zirconia phases and the ε-Co(1 1 1) peak showing an intensity comparable to that obtained for R1000. No peak corresponding to carbon is detected. The carbon content is equal to 3.7 wt%. The specific surface is equal to 7.9 m^2/g. FEG-SEM and TEM observations (Fig. 7) reveal many different carbon species, including short carbon nanofibers, nanoribbons, hollow particles often forming bamboo structures, carbon-encapsulated Co particles and CNTs, albeit in a fairly low proportion. This is by and large similar to what is reported when using a ZrO_2-supported Fe catalyst [15]. The selectivity towards the formation of CNTs is far less than what is obtained using a $Mg_{0.9}Co_{0.1}O$ solid solution as starting material, the reduction of which provokes mainly the formation of single- and double-walled CNTs [14] and less than what is obtained using a $Mg_{0.9}Co_{0.1}Al_2O_4$ solid solution as starting material [13]. The formation of so many different carbon species upon reduction is known to reflect that the catalytic material is prone to the formation of metal particles with a large or even multimodal size distribution and a fairly high average size [13,22,23], well above the 3–5 nm cutoff size [24,25] for the formation of CNT. The propensity of the present catalytic material to form too large Co particles is thought to arise because of the relatively poor thermal stability of the solid solution and possibly because the Co^{2+} ions are not diluted enough in the zirconia lattice. In both cases, using lower cobalt content could be beneficial.

In the following part of the study, it was attempted to perform the reduction at a much lower temperature (650 °C) in order to obtain a lower amount of metallic phase through a lower reduction rate of the Co^{2+} ions, which would favor the formation of smaller Co particles. The lower temperature would also help in avoiding their coalescence. Since the catalytic decomposition of CH_4 is fairly low at 650 °C, the tetragonal $Zr_{0.9}Co_{0.1}O_{1.9}$ solid solution was reduced in H_2–C_2H_4 atmosphere (40 mol.% C_2H_4). The XRD pattern (not shown) presents the peaks of tetragonal zirconia as well as a very wide ε-Co(1 1 1) peak with a very weak intensity. No peak corresponding to carbon is detected. The carbon content is equal to 16.3 wt% and the specific surface is equal to 36.3 m^2/g. Interestingly, both values are over four times what is obtained for the powder reduced in H_2–CH_4 at 1000 °C. At least part of specific surface area increase compared to the starting solid solution (23.7 m^2/g) could correspond to the formation of some filamentous carbon species. FEG-SEM and TEM observations (Fig. 8) reveal the presence of carbon filaments with a diameter in the range 15–30 nm. Although some larger nanofibers can be observed in some areas, the powder reduced in H_2–C_2H_4 is quite different and much more homogeneous than the one reduced in H_2–CH_4. Some filaments show some degree of branching and some of them do not appear to be hollow (Fig. 8c). The tip of some filaments contains a particle, probably cobalt, appearing as dark dots in Fig. 8c. These carbon filaments resemble those obtained by heat-treatment of Fe/Ni-Al_2O_3 catalysts at 650 °C in N_2–C_2H_4 (17%C_2H_4) [26] or Fe_2O_3-based catalysts in H_2–C_2H_4 [27], although

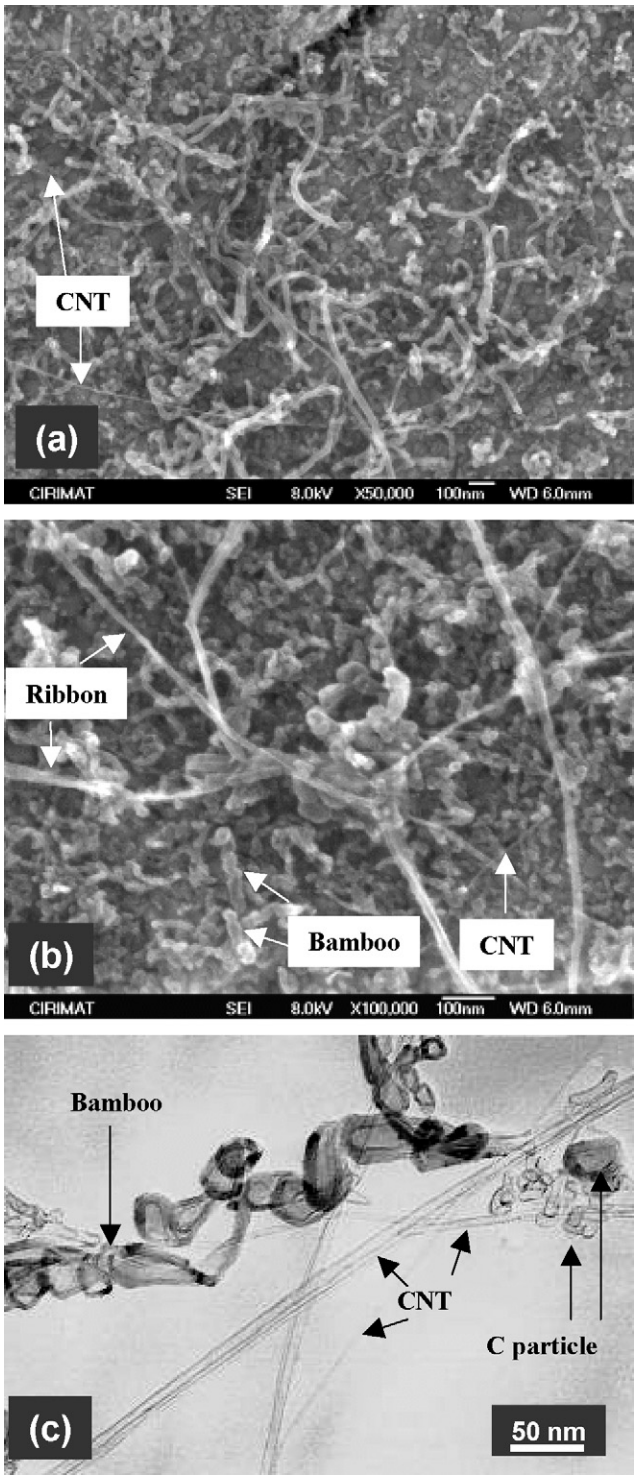

Fig. 7. FEG-SEM images (a, b) and TEM image (c) of the powder prepared by reduction in H_2–CH_4 at 1000 °C.

their diameter is significantly smaller (15–30 nm vs. over 100 nm). Those filaments that are not hollow could be identified as the so-called platelet nanofibers, where the graphene sheets are parallel to each other and are perpendicular to the direction of the axis of the filament [28]. Interestingly, McCaldin et al. [27] showed that the formation of the various carbon forms (platet nanofibers, herrinbone nanofibers, multi-walled CNTs and encapsulated

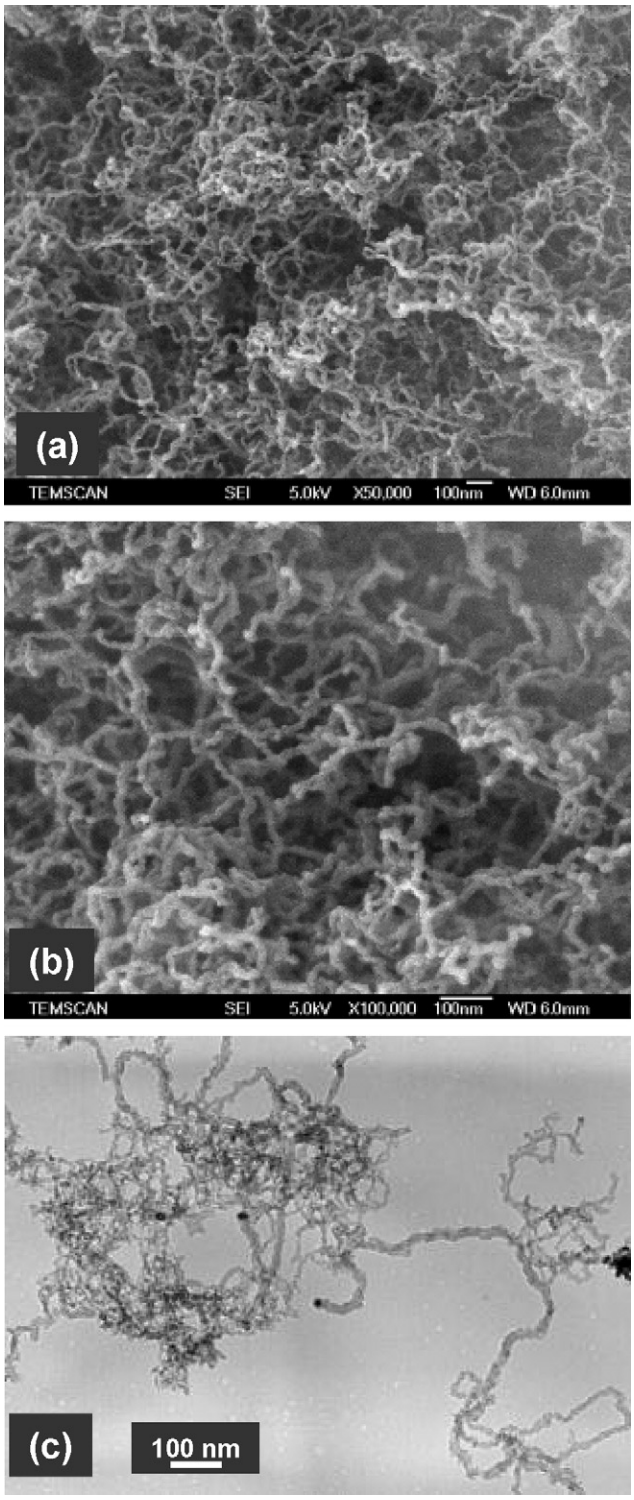

Fig. 8. FEG-SEM images (a, b) and TEM image (c) of the powder prepared by reduction in H_2–C_2H_4 at 650 °C.

metal particles) was strongly depending on the temperature (400–800 °C) and H_2–C_2H_4 gas mixture composition. The present experimental conditions (650 °C, 40% C_2H_4) are just outside the temperature-composition space (both on the high-side) for which they report the formation of the platelet nanofibers, but this probably reflects the difference in catalytic material. Thus, in order to principally obtain the carbon as multi-walled CNTs, future studies will be devoted to fine tuning some materials characteristics such as the nature of the catalyst metal (Co, Fe, Ni or alloys), its proportion with respect to ZrO_2 and the stabilization of ZrO_2 by a non-reactive oxide such as Y_2O_3. Some reaction parameters such as temperature, duration and gas composition and flow rate will also be investigated. As noted by Ferlauto et al. [16], such CNT–metal–ZrO_2 composites could be interesting due to mixed electronic-ionic transport properties.

4. Conclusions

The synthesis of a $Zr_{0.9}Co_{0.1}O_{1.9}$ solid solution fully stabilized in tetragonal form is reported for the first time. The nitrate/urea combustion route was used and it is shown that the appropriate amount of urea is seven times the so-called stoichiometric proportion. A study of the thermal stability in air revealed that the phase partitioning from the cobalt-stabilized tetragonal solid solution to the mixture of *m*-ZrO_2 and Co_3O_4 takes place at temperatures as low as 625 °C. A study of the reduction of the $Zr_{0.9}Co_{0.1}O_{1.9}$ solid solution in H_2, H_2–CH_4 and H_2–C_2H_4 atmospheres indicated that the Co particles formed upon reduction are probably of a too large size, and size distribution, to be selective towards the formation of single- and double-walled CNTs. In particular, reduction at 1000 °C in H_2–CH_4 produced many carbon species including short carbon nanofibers, nanoribbons, hollow particles often forming bamboo structures, carbon-encapsulated Co particles and CNTs. By contrast, reduction at 650 °C in H_2–C_2H_4 produced 15–30 nm nanofibers. For at least some of them, the graphene sheets are parallel to each other and are perpendicular to the direction of the axis of the filament. Future studies will be devoted to fine tuning both some materials characteristics and some reaction parameters in order to improve the selectivity towards CNTs.

Acknowledgments

The authors would like to thank Mr. L. Datas and Mr. L. Weingarten for their assistance in the TEM observations, which were performed at TEMSCAN, the ''Service Commun de Microscopie Electronique à Transmission'', Université Paul-Sabatier.

References

[1] L.A. Boot, M.H.J.V. Kerkhoffs, B.T. van der Linden, A.J. van Dillen, J.W. Geus, F.R. van Buren, Appl. Catal. A 137 (1996) 69–86.
[2] T.-C. Xiao, S.-F. Ji, H.-T. Wang, K.S. Coleman, M.L.H. Green, J. Mol. Catal. A 175 (2001) 111–123.
[3] V.G. Milt, M.A. Ulla, E.A. Lombardo, J. Catal. 200 (2001) 241–249.
[4] V.G. Milt, E.A. Lombardo, M.A. Ulla, Appl. Catal. B 37 (2006) 63–73.
[5] M. Kantcheva, A.S. Vakkasoglu, J. Catal. 223 (2004) 364–371.
[6] V.R. Choudhary, S. Banerjee, S.G. Pataskar, Appl. Catal. A 253 (2003) 65–74.
[7] I.D. Lick, A. Carrascull, M. Ponzi, E.N. Ponzi, I.L. Botto, Mater. Chem. Phys. 92 (2005) 327–332.
[8] P. Soisuwan, P. Praserthdam, J. Panpranot, D.L. Trimm, Catal. Commun. 7 (2006) 761–767.
[9] M. Yashima, T. Hirose, S. Katano, Y. Suzuki, M. Kakihana, M. Yoshimura, Phys. Rev. B 51 (1995) 8018–8025.
[10] F. Maglia, U. Anselmi-Tamburini, G. Spinolo, A.J. Munir, Mater. Synth. Process. 7 (1999) 327–332.
[11] A. Ringuede, J.A. Labrincha, J.R. Frade, Solid-State Ionics 141–142 (2001) 549–557.
[12] F. Legorreta Garcia, V. Gonzaga de Resende, E. De Grave, A. Peigney, A. Barnabé, C. Laurent, Solid-State Ionics, submitted for publication.
[13] A. Govindaraj, E. Flahaut, C. Laurent, A. Peigney, A. Rousset, C.N.R. Rao, J. Mater. Res. 14 (1999) 2567–2576.
[14] E. Flahaut, A. Peigney, C. Laurent, A. Rousset, J. Mater. Chem. 10 (2000) 249–252.
[15] M.A. Ermakova, D.Y. Ermakov, A.L. Chuvilin, G.G. Kuvshinov, J. Catal. 201 (2001) 183–197.
[16] A.S. Ferlauto, D.Z. Deflorio, F.C. Fonseca, V. Esposito, R. Muccillo, E. Traversa, L.O. Ladeira, Appl. Phys. A 84 (2006) 271–276.
[17] S. Kurasawa, S. Iwamoto, M. Inoue, Mol. Cryst. Liq. Cryst. 387 (2002) 123–128.
[18] K.C. Patil, Bull. Mater. Sci. 16 (1993) 533–541.
[19] Y. Zhang, G.C. Stangle, J. Mater. Res. 9 (1994) 1997–2004.
[20] R.C. Garvie, P.S. Nicholson, J. Am. Ceram. Soc. 55 (1972) 303–305.
[21] V. Gonzaga de Resende, F. Legorreta Garcia, A. Peigney, E. De Grave, C. Laurent, Solid-State Ionics, submitted for publication.
[22] Ch. Laurent, A. Peigney, A. Rousset, J. Mater. Chem. 8 (1998) 1263–1271.

[23] P. Coquay, A. Peigney, E. De Grave, R.E. Vandenberghe, C. Laurent, J. Phys. Chem. B 106 (2002) 13199–13210.
[24] J.H. Hafner, M.J. Bronikowski, B.R. Azamian, P. Nikolaev, A.G. Rinzler, D.T. Colbert, K.A. Smith, R.E. Smalley, Chem. Phys. Lett. 296 (1998) 195–202.
[25] A. Peigney, P. Coquay, E. Flahaut, R.E. Vandenberghe, E. De Grave, Ch. Laurent, J. Phys. Chem. B 105 (2001) 9699–9710.
[26] W. Qian, T. Liu, Z. Wang, H. Yu, Z. Li, F. Wei, G. Luo, Carbon 41 (2003) 2487–2493.
[27] S. McCaldin, M. Bououdina, D.M. Grant, G.S. Walker, Carbon 44 (2006) 2273–2280.
[28] W.B. Downs, R.T.K. Baker, J. Mater. Res. 10 (1995) 625–633.